Journal of *Marine Science and Engineering*

MDPI

Article

Three-Dimensional Binary Marker: A Novel Underwater Marker Applicable for Long-Term Deployment Scenarios

Alaaeddine Chaarani [1,*], Patryk Cieslak [1], Joan Esteba [2], Ivan Eichhardt [3] and Pere Ridao [1]

[1] Computer Vision and Robotics Research Group (ViCOROB), Universitat de Girona, UDG, 17003 Girona, Spain; patryk.cieslak@udg.edu (P.C.); pere.ridao@udg.edu (P.R.)
[2] Center for Artificial Intelligence and Robotics (CAIR), New York University Abu Dhabi, NYUAD, Abu Dhabi P.O. Box 129188, United Arab Emirates; joan.esteba@nyu.edu
[3] Department of Algorithms And Their Applications, Eötvös Loránd University, ELTE, 1064 Budapest, Hungary; ivan.eichhardt@gmail.com
* Correspondence: u5501938@udg.edu

Abstract

Traditional 2D optical markers degrade quickly in underwater applications due to sediment accumulation and marine biofouling, becoming undetectable within weeks. This paper presents a Three-Dimensional Binary Marker, a novel passive fiducial marker designed for underwater Long-Term Deployment. The Three-Dimensional Binary Marker addresses the 2D-markers limitation through a 3D design that enhances resilience and maintains contrast for computer vision detection over extended periods. The proposed solution has been validated through simulation, water tank testing, and long-term sea trials for 5 months. In each stage, the marker was compared based on detection per visible frame and the detection distance. In conclusion, the design demonstrated superior performance compared to standard 2D markers. The proposed Three-Dimensional Binary Marker provides compatibility with widely used fiducial markers, such as ArUco and AprilTag, allowing quick adaptation for users. In terms of fabrication, the Three-Dimensional Binary Marker uses additive manufacturing, offering a low-cost and scalable solution for underwater localization tasks. The proposed marker improved the deployment time of fiducial markers from a couple of days to sixty days and with a range up to seven meters, providing robustness and reliability. As the marker survivability and detection range depend on its size, it is still a valuable innovation for Autonomous Underwater Vehicles, as well as for inspection, maintenance, and monitoring tasks in marine robotics and offshore infrastructure applications.

Keywords: localization; underwater; Three-Dimensional Binary Marker (3D-BM); passive markers

check for updates

Academic Editor: Weicheng Cui

Received: 26 June 2025
Revised: 18 July 2025
Accepted: 24 July 2025
Published: 28 July 2025

Citation: Chaarani, A.; Cieslak, P.; Esteba, J.; Eichhardt, I.; Ridao, P. Three-Dimensional Binary Marker: A Novel Underwater Marker Applicable for Long-Term Deployment Scenarios. *J. Mar. Sci. Eng.* **2025**, *13*, 1442. https://doi.org/10.3390/jmse13081442

Copyright: © 2025 by the authors. Licensee MDPI, Basel, Switzerland. This article is an open access article distributed under the terms and conditions of the Creative Commons Attribution (CC BY) license (https://creativecommons.org/licenses/by/4.0/).

1. Introduction

Underwater Unmanned Vehicles (UUV's) are routinely used for marine science, energy, defense, and commercial applications. Autonomous Underwater Vehicles (AUVs) are commonly used to explore an area of interest using multimodal sensors (multibeam sonar profilers, side-scan sonar, imaging sonars, monocular or stereo cameras, etc.) to gather data which are used later on for cartography (bathymetry, sonar mosaics, photogrammetry, etc.). Normally, these applications take place in predominantly flat terrains, where AUVs fly at constant altitude. Nevertheless, there are other applications related to the Inspection, Maintenance, and Repair operations, commonly performed on offshore infrastructure, where the UUV has

to move close to 3D structures either to inspect them or to manipulate them. These types of operations are nowadays done with Remotely Operated Vehicles (ROVs).

In recent years, there has been an interest in automatizing these types of operations, evolving from the intervention ROV concept to the intervention AUV intervention (I-AUV) one [1]. To achieve this, it is necessary to localize the I-AUV with very high accuracy with respect to the infrastructure, which can only be achieved using optical sensors. Though the ultimate interest is to be able to solve the problem using generic methods such as visual SLAM, it is very interesting to have simpler alternatives that are easy to deploy and use.

Optical markers have proven to be very useful for these tasks in other robotic domains, including industrial, mobile, and aerial robotics. For this reason, they have also started to be used in underwater robotics, particularly in proof-of-concept demonstrations performed in water tanks. Unfortunately, traditional 2D fiducial markers (e.g., ArUco [2], AprilTag [3]) degrade rapidly underwater due to sediment accumulation and biofouling, obscuring their binary patterns within weeks. Flat surfaces exacerbate fouling, while turbidity and light scattering further reduce detectability, as mentioned in Section 2. These limitations hinder Long-Term Deployment for AUV. In practical experiments, when we need to increase the Technology Readiness Level, transitioning from the water tank to sea trials, the conventional optical markers fail after a short time due to the accumulation of sediments and the growth of biofouling.

The previous reasons inspired this research work, whose goal is to present an extension to the state-of-the-art optical markers to make them more robust for field applications, becoming more resilient to the deposition of sediments and the growth of biofouling.

The paper is organized as follows. Section 2, provides a quick summary of the state of the art for underwater markers. Section 3 presents the methodology used to develop the proposed marker, and Section 5 shows the field results during a long-term trial at sea. Finally, in Section 6, a summary of the paper is provided together with the concluding remarks.

2. State of the Art

Optical fiducial markers are commonly used nowadays for any robotic problem that can be formulated as a camera pose estimation. This includes problems like robot localization, object localization, or object tracking, to name some of them.

Markers can be active (they emit their own light) [4] or passive (they reflect the received light). The effects of noise on active and passive markers were studied in [5], concluding that active markers are less affected by light absorption and scattering underwater. The authors also pointed out the need to improve passive markers as a cheap and simple solution for many underwater applications.

The most-used passive markers are the fiducial ones that share a square flat pattern with a black border and several square bits, which simplifies their detection, following some codification. Several survey papers have been published about this subject. A good qualitative and quantitative evaluation of some of the most relevant marker systems is reported in [6], where the authors analyze their differences and limitations, and conduct detailed experiments to compare them in terms of sensitivity, specificity, accuracy, computational cost, and performance under occlusion. Another good comparative study is presented in [7], which compares the accuracy, detection rate, and computational cost in several scenarios that include simulated noise from shadows and motion blur, focusing on four widely used markers, Figure 1 (ARTag [8], AprilTag [3], ArUco [2], and STag [9]). Since these markers perform well for terrestrial and aerial applications, in recent years, there has been a significant effort to use them in underwater applications. Saipem [10] used the AprilTag [3] in their vehicles (FlatFish, Hydrone-R, and Hydrone-W). Typical applications include visual docking [11,12], single vehicle vision-based navigation [13,14],

and swarm localization [15]. Nevertheless, the underwater domain poses new challenges due to the inherent constraints of light propagation through the water. A comparative study of Apriltags, ArUco, and ARToolkit operating underwater was reported in [16]. The authors performed several experiments to compare the performance of the markers at different turbidity levels and lighting conditions.

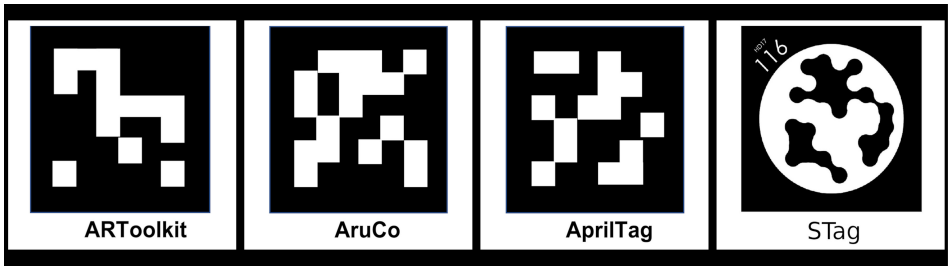

Figure 1. Displays an example of fiducial Markers.

There have been some attempts to improve the performance of passive markers underwater. Some authors have proposed an enhancement for the perception of visual markers through active exposure control [17]. Others [18] have proposed methods to improve the light reflection using retro-reflective material to increase the detection and the range of visibility. Cejka et al. proposed the UWARUco marker as an adaptation of the standard ArUco marker to the underwater environment [19]. Their algorithm replaces the ArUco detection method, which reduces the number of contours caused by noise, with a method that masks out areas that do not contain any markers. Cesar et al. proposed an improvement to the marker detection front-end by pre-processing the image before feeding it to the detection algorithm [20]. They tested different methods of image enhancement, including Contrast-Limited Adaptive Histogram Equalization (CLAHE) and min/max normalization on greyscale images, which boost the marker detection.

Unfortunately, none of the methods described above are robust against the accumulation of sediments, nor against marine biofouling, which are common problems that appear when moving from the lab (water tank) to the sea. The problem of marine fouling could be partially mitigated with the anti-biofouling signalling technology currently used for labelling offshore infrastructure [21] or by a copper layer [22]. Unfortunately, there is still no solution for sediment accumulation, which is very serious in shallow water environments. This paper proposes a new method of constructing fiducial markers that significantly improves their robustness against fouling and sediment deposited on the markers. The method takes advantage of a 3D relief that can be easily obtained by conventional 3D printing. This article reports Long-Term Deployment results compared to state-of-the-art solutions.

3. The Underwater 3D Marker

The marker development is divided into four main stages: conception, simulation, validation in a controlled environment, and testing in a real environment.

3.1. Requirements

We are interested in designing a marker for Long-Term Deployment underwater that is easily detectable, able to provide the camera pose, and robust to marine growth and sediment accumulation. Therefore, the following requirements apply:

1. Optical: The proposed marker should be easily detectable using computer vision.
2. Passive: The proposed marker should not require energy to be operative, therefore promoting Long-Term Deployment.

3. Observable: When detected, it should be able to provide the camera pose from a single observation.
4. Binary: To improve the detection, even in poor light conditions, a binary black and white marker will be used. Avoiding the use of color will promote robustness, since it is known that the perception of color underwater is affected by wavelength-dependent attenuation [23].
5. Robust to marine growth and sediments: Marine growth and sediments are the main challenges in Long-Term Deployment as they cover the objects, occlude the pattern, and change the contour of geometrical features. Flat surfaces facilitate the accumulation of sediments, which needs to be avoided or at least minimized.

3.2. Three-Dimensional Binary Marker Underwater Marker Proposal

Most of the requirements proposed above are already satisfied by optical fiducial markers (Figure 1) such as ArUco [2], the ARTOOLKIT [8], or the AprilTag [3]. All of them are optical, passive, binary tags able to provide camera poses through a single observation. Therefore, the key property here is the resilience against marine growth and sediments accumulated over time.

Fiducial tags use the contrast between black and white squares to facilitate detecting features during localization. Figure 2 shows a regular fiducial marker (the one in the middle) underwater on its deployment day, 20, and 45 days later. Although the marker is clearly detectable in Figure 2a, it is hardly recognizable in Figure 2c. The problem arises after a few days of deployment, from the accumulation of sediments as well as from the marine growth. The fact that the marker is made of a completely flat surface facilitates the accumulation of dirt.

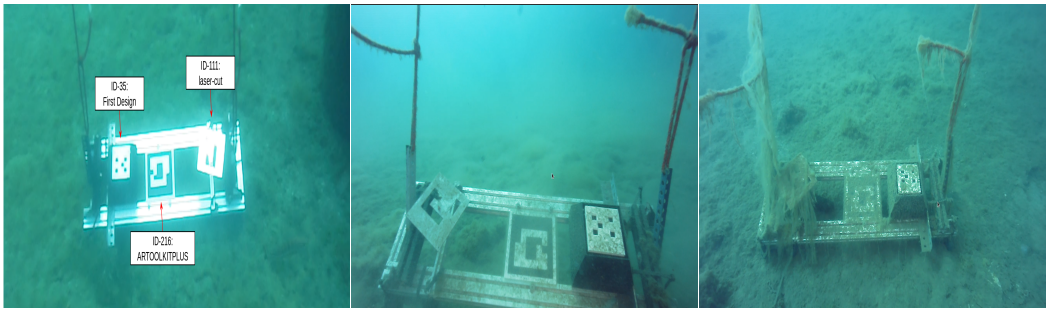

(**a**) Deployment day (**b**) 20 days of deployment (**c**) 45 days of deployment

Figure 2. Example of the effect of sediments and marine growth over 45 days of underwater deployment, sea experiment 1.

Our proposal, to make it robust against sediments and marine growth, is to build it in 3D (Figure 3). Therefore, the proposed Three-Dimensional Binary Marker (3D-BM) is an extension of the binary tag from two to three dimensions. This is done by dividing the binary marker into two main parts: the binary pattern and the enclosure. The enclosure creates a controlled background for the binary pattern, which reduces the effect of the reflected light. The enclosure holds the pattern at a certain distance from the back layer and creates enough space to diminish entering light. This generates a contrast between the two layers of the marker. This design is manufactured using additive manufacturing, which facilitates the testing process. Figure 4, shows the proposed prototypes.

This concept design allows for the extension of any existing flat fiducial market into its 3D counterpart. For instance, in the case of extending a 2D ArUco to 3D, the obtained Underwater Marker is referred to as Three-Dimensional ArUco Marker (3D-AM).

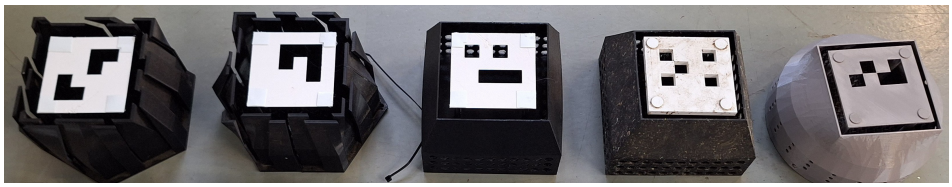

Figure 3. All the Three-Dimensional ArUco Marker used in the experiments, with hexagon, square, and circular enclosures.

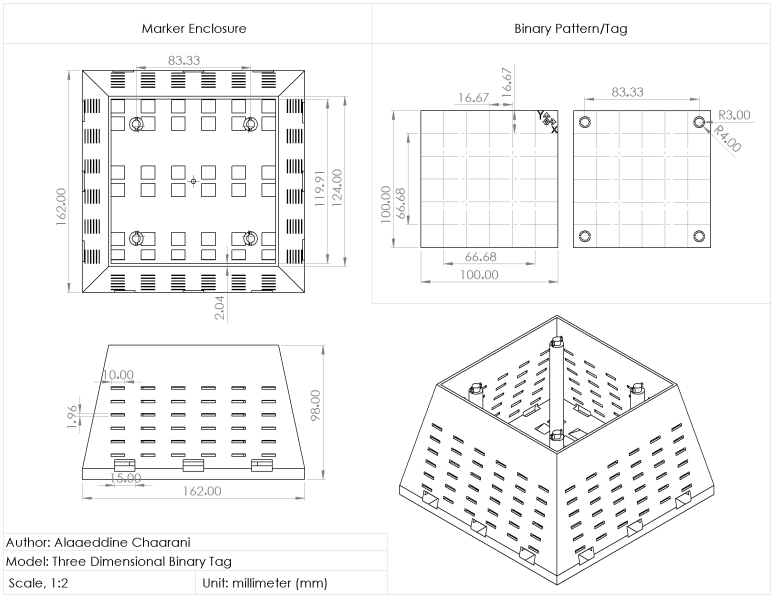

Figure 4. 3D-BM CADModel, square-shaped enclosure, the final design.

The reuse of this design can be done in any form that provides enough spacing for the binary pattern. There should be an enclosure to allow the entrance of light from the front layer and to prevent any confusion with surrounding objects. Also, the front layer (binary pattern) needs to be thin to allow proper detection when observed diagonally. The proposed Three-Dimensional Binary Marker has the following dimensions (Figure 4):

- Enclosure shape: We proposed three shapes for the enclosure, which were the square, circle, and hexagon, Figure 3. Considering that the pattern contour and the enclosure's external contour could be confused, this categorical parameter was checked to see if it has any effect on the detection.
- Enclosure height: A space of 10 cm between the enclosure and the pattern gives enough space for the light to decay in the enclosure.
- Binary pattern dimension: Regardless of the library used to generate the binary pattern, there should be a clearance space of 1 cm between the enclosure and the binary pattern. The side length is 10 cm and 1 mm thick. In case of increasing or decreasing the size of the enclosure, the dimensions of the pattern and the enclosure should be correlated. Note that we refer in a generic way to the 3D binary tag as 3D-BM. When the tag is an ArUco tag, we refer to it as 3D-AM-XX, being XX its ID code.
- Marker color: To facilitate the detection, the binary pattern is manufactured using bright colors (i.e., white) while the marker enclosure is manufactured using dark colors (i.e., black). This color distribution is the inverse of the standard fiducial markers' colors.
- Enclosure internal pattern: The internal pattern helps to create the contrast between the front binary layer and the back layers of the enclosure. This idea is inspired by the anechoic chamber [24]. The internal background of the enclosure was filled with a 2 cm long triangular pattern, Figure 3.

3.3. Three-Dimensional Binary Marker Detection Algorithm

The 3D binary marker is actually a 3D extension of existing fiducial markers or binary tags like ArUco [2], AprilTag [3], or ArToolKitPlus [8]. This allows the use of existing detection algorithms, often available in the OpenCV library [25]. However, this proposed design requires pre-processing the acquired images. The process can be divided into two steps: (1) image pre-processing, which prepares the Three-Dimensional Binary Marker to be recognized by the detection algorithm, and (2) binary tag detection with camera-pose estimation. During the pre-processing, the image is treated and enhanced to improve the detection probability.

A preliminary set of pre-processing methods was considered, including: (1) convolution blur kernels followed by a binarization [26]; (2) fixed and dynamic threshold binarization [27], iterative threshold binarization; (3) morphic operations, dilation/erosion after binarization with different kernel sizes and morphic shapes [28]; (4) min-max normalization, sharpening and blur convolution; and (5) CLAHE using min/max normalization and blur convolution. These pre-processing methods were applied to the rendered dataset. The methods with lower detection rates than the simple normalization method were discarded, leaving only the next three methods for final comparison (Figure 5):

- CLAHE with normalization: First, CLAHE is applied to get an image with a better local contrast between the front and back layers of the marker. Next, the image is inverted and normalized using min/max normalization. The inversion is required as the Three-Dimensional Binary Marker colors are an inversion of the original fiducial colors. The normalization accounts for the pixel intensity variation, common in underwater images, due to the lighting and water conditions, as well as the distance to objects. Finally, a convolution blur with a 3×3 kernel is applied to enhance the detection of the pattern contours.
- Iterative Binarization: It uses an inverse threshold with ranges between 0 and 255, then a convolution blur. The threshold is changed iteratively in steps of 5 units while processing an image, selecting the one generating the highest number of successful marker detections.
- Normalization: This method applies min/max normalization to the image, and then inverts the image values.

Once the image has been preprocessed, it is used as input to the conventional marker detection algorithm.

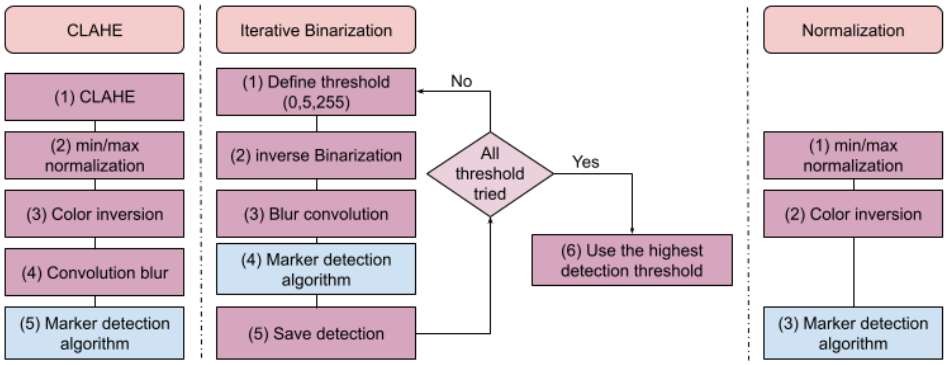

Figure 5. Flowcharts for the three chosen detection algorithms.

4. Validation

The validation process aims to evaluate the proposed designs based on the criteria established in Section 3.2 and ensure their detectability over time.

Therefore, a validation methodology based on three steps was established: (1) simulation, (2) water tank testing, and (3) sea trials.

4.1. Simulation

Simulation was used to ensure the reliability of the proposed marker and its detection algorithm in virtual conditions. Using Blender software [29], we generated several videos (500–700 frames) of a submerged Docking Station equipped with Three-Dimensional Binary Marker markers (see Figure 6b).

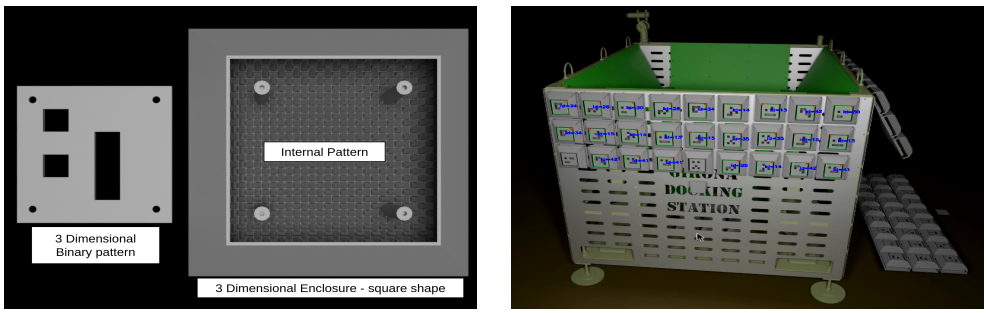

(**a**) Three-dimensional BM square model for simulation

(**b**) Three-dimensional BM validation test in simulation

Figure 6. Shows the Three-Dimensional Binary Marker marker design for simulating a sample of the simulation validation, and the final produced shape.

4.2. Water Tank Testing

The second step was used to test the Three-Dimensional Binary Marker using a Remotely Operated Vehicle operated in a water tank controlled environment. Though this is the first experimental test, it takes place in crystal-clear waters. So it only provides a first insight into the potential possibilities of the proposal and allows checking the experimental methodology before time-consuming field trials.

4.3. Sea Trials

In this step, the structures shown in Figures 2a and 8 were deployed in Sant Feliu de Guixols harbour (Spain) at a depth of 10 m. An Remotely Operated Vehicle, equipped with a forward-looking camera, performed a trajectory while detecting the markers (Figure 7). This trajectory included static observations, linear surge movement, and sway motion while rotating around the structure. The trajectory was carried out repeatedly at altitudes of 1, 2, 3, 4, and 5 m from the sea bed.

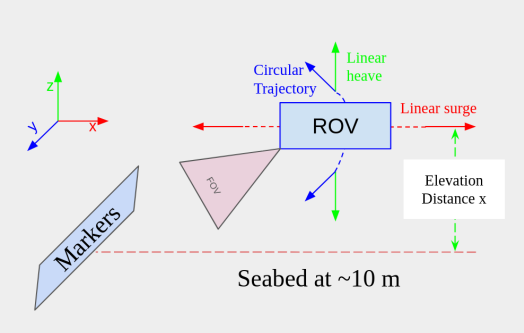

Figure 7. Aluminium structure equipped with markers, submerged in Sant Feliu harbour.

We intended to have multiple recordings of the deployed structure to evaluate the detectability over deployment time. These recordings are spread apart to have enough time for sea sediments to accumulate. The first visit after the deployment was scheduled in

three weeks, while the other visits are two weeks after. The experiment ends if the Three-Dimensional Binary Marker loses detectability or if it successfully performs better than the Standard ArUco Marker. The evaluation is done using two methods. (1) By averaging the detection percentage of each marker, and (2) by comparing the Three-Dimensional ArUco Marker or other markers detection rate to the Standard ArUco Marker detection rate.

Although the trajectories the Remotely Operated Vehicle performed on different days throughout the deployment period were intended to be the same, they differ slightly, as the vehicle was driven manually. Therefore, the number of markers appearing in the field of view differs between videos. In order to make a consistent comparison between the sets of videos collected, we only processed frames in which all deployed markers were visible within the field of view, with a size sufficient for them to be detectable. Two different field trials were conducted:

1. Short Term Deployment Experiment: This was a 45-day deployment experiment involving only three markers (Figure 2) having different material and conceptual designs: (1) an Standard ArUco Marker; (2) a Lazer cut ArUco Marker, and (3) the proposed 3D ArUco marker (3D-AM). The goal of this experiment was to have a quick assessment of the most promising type of marker. The results of this experiment are reported in Section 5.3.
2. Long-Term Deployment Experiment: This was a 5-month deployment experiment (Figures 8 and 11) that used the same three types of markers presented in the Short Term Experiment, but all of them were manufactured using the same material and the same pattern size. The goal was to compare the detection capabilities of each marker type over time to determine the most effective one. For this reason, we considered different configurations, including (1) different inclination angles, (2) separation distances between the pattern and the background, (3) different enclosure internal patterns, and (4) different enclosure shapes.

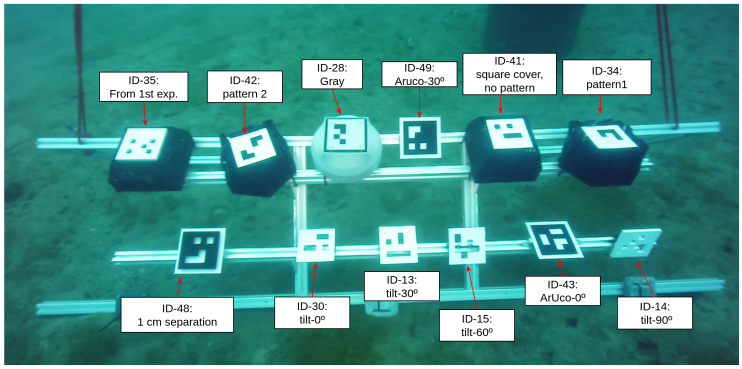

Figure 8. Shows the experiment 2 structure on the first day of deployment.

In this experiment, the structure was equipped with twelve different markers. The 3D-AM-35 already used in the previous experiment was included to compare with the 3D-AM-34, 3D-AM-41, and 3D-AM-42, which have an improved binary pattern and enclosure design. The 3D-AM-28, a full gray marker, was used to prove the concept of generating contrast from shape. Since the pattern and the cover are gray, the generated marker is created by the shape, while the color has minimal effect on the detection of the marker. Standard ArUco markers, ST-AM-49 and ST-AM-43, were also included, each one with a different tilt angle, to check the effect of sediment accumulation. The Lazer cut ArUco Marker ID:13-14-15-30, each was tilted with an angle, to be observed and compared for the accumulation of sediments based on tilt. Finally, an ArUco marker with ID 48 (ST-AM-48-Split), with a 1 cm distance between

the pattern and the background, was included to validate the need for the enclosure and the 10 cm depth. The results of this experiment are presented in Section 5.4.

5. Results

Following the validation procedures detailed in Section 4, this section presents the results obtained from the simulation, test tank, and sea environment experiments. Each stage of validation has provided critical insights into the performance and robustness of the 3D-BM marker. The results highlight how the marker responds to environmental factors such as sediment accumulation and marine growth over time, and how design refinements—guided by earlier validation steps—have improved its detectability. Detection rates and the impact of different pre-processing techniques are analyzed, demonstrating the effectiveness of the proposed 3D design in real-world underwater conditions.

5.1. Three-Dimensional AT Simulation

The evaluation of the pre-processing method and design was done by comparing the number of detections achieved. In each scene, we modified different parameters, including marker size, marker ID, enclosure shape, and clearances. Some of these parameters had a slight effect on the detection (e.g., internal pattern and external shape of the enclosure, marker ID, pattern surface, incident light, and some others), so we didn't evaluate further. while other parameters were significant (e.g., clearance space between pattern and enclosure, enclosure internal depth, and marker size), which is evaluated more in the sea experiments.

These tests allowed the narrowing down of the pre-processing methods to three methods (CLAHE, iterative threshold, and normalization). They also provided the authors with the first design of the Three-Dimensional Binary Marker that was manufactured and used in the test tank and sea evaluation.

5.2. Three-Dimensional AM in Controlled Environment

Using an Remotely Operated Vehicle, the 3D-AM marker was recorded in the test tank. The recorded video results in 9168 frames, in which the 3D-AM marker was detected in 68% of the frames with a distance up to six meters, Figure 9.

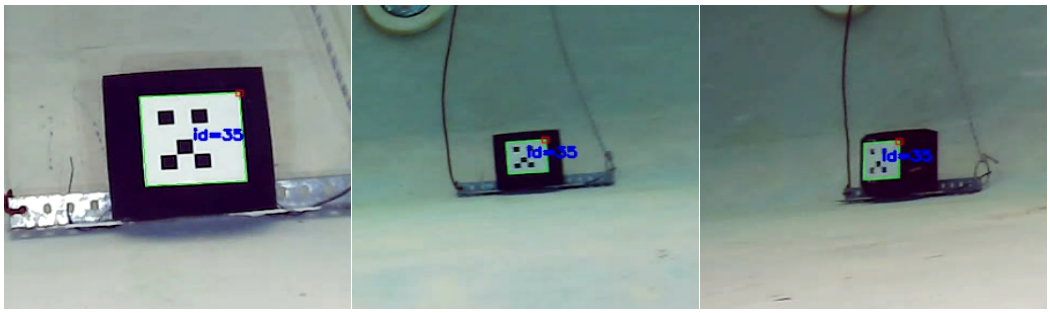

(**a**) Front view, close (**b**) Front view ∼ 4m (**c**) Side view

Figure 9. Detection applied on the proposed marker in the test tank, Three-Dimensional ArUco Marker: ID-35.

5.3. Experiment I: Short Term Validation Experiment

In this experiment, we submerged a structure (Figure 2a) made of an aluminum frame where three different markers were mounted: (1) a tilted laser-cut ArUco Marker with ID 111 (LC-AM-111), (2) a horizontal standard ArUco Marker with ID 216 (ST-AM-216), and (3) a horizontal 3D ArUco Marker ID 35 (3D-AM-35). The videos are recorded on deployment day(Figure 2a), 20 days later (Figure 2b), and 45 days after deployment (Figure 2c).

From the first two recorded videos, we plotted Figure 10 to show the detection percentage of each of the markers and compare it. On the day of deployment, the detection of the standard ArUco marker (ST-AM) was slightly higher than the detection of the proposed 3D marker (3D-AM) (42.1% vs 36.2%), Figure 10a. This difference can be attributed to its larger size (14 × 14 cm vs 10 × 10 cm), which makes its detection easier. Twenty days later, Figure 10b, the 3D-AM performed better than the ST-AM (57.6% vs 21.6%), showing its resilience to dirt and marine growth. After 45 days of deployment, the standard marker was not detectable anymore, while it was still possible to detect the 3D marker at 1.5 to 2.5 m range using the iterative threshold method. The laser-cut marker (LC-AM) was never detected in any of the experiments.

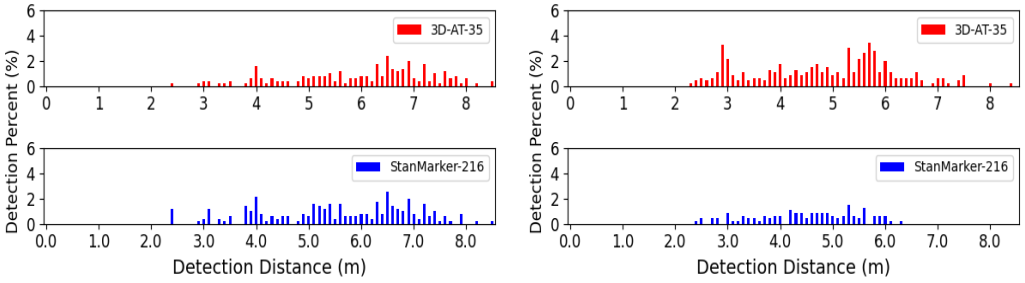

(**a**) 1st day (**b**) 20th day

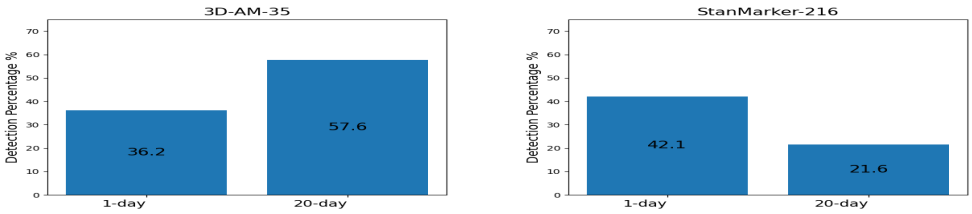

(**c**) Detection percentage of the 3D-AM (**d**) Detection percentage of the ST-AM

Figure 10. Shows the detection percentage and the pose estimation of the deployed structure over the course of 20 days.

After the first experiment, it was decided to increase the gap between the enclosure and the binary pattern in order to provide more space between the edges. This increased the time required by the marine growth to cover the marker pattern, augmenting the resilience. Another improvement was the decrease in the binary pattern thickness from 5 mm to 1 mm. This prevented the visualization of the pattern's side when observed diagonally. With a 5 mm thickness, the binary pattern side leads to detection failure due to the variability in the black-and-white spacing ratio.

From this experiment, we concluded that the proposed 3D-AM markers have the potential to improve the percentage of marker detections as time passes and they get dirtier and covered by sediments.

5.4. Experiment II: Long-Term Validation Experiment

In this case, the structure shown in Figure 8 was submerged and five video datasets were collected (Figures 8 and 11a–d) over 5 months. Figure 12 shows the detection percentage for each dataset and each pre-processing method (CLAHE, iterative threshold, and normalization). Note that for the ST-AM markers, only the normalization pre-processing was used, since this is the standard procedure.

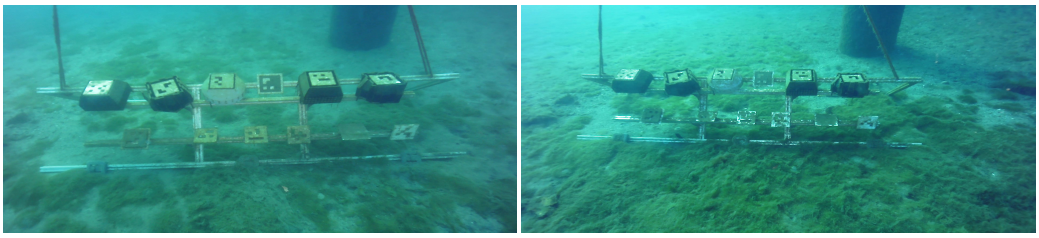

(**a**) 21 days after deployment (**b**) 35 days after deployment

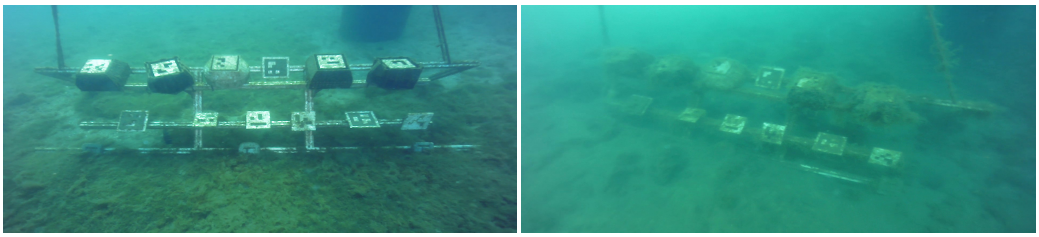

(**c**) 50 days after deployment (**d**) 120 days after deployment

Figure 11. Marker status over 5 months of deployment. Deployment day is presented in Figure 8.

5.4.1. Detectability Improvement

Results shown in Figure 12a–e correspond to 3D markers, while results shown in Figure 12f–h correspond to standard ones. It can be appreciated that, in general, the 3D markers are detectable along the four datasets with the exception of the first one (3D-AM-35), which is included for reference only. This one, which is detectable on the first day but suffers difficulties on the following days, corresponds to the former design used in Experiment I. The rest of the 3D markers (Figure 12b–e) include the improvements suggested after experiment I, and their performance is consistent over the days. The markers are detectable along all the datasets, with detection percentages decreasing as time passes and dirt accumulates. The standard markers work fine on the deployment day, but their performance decays quickly over time.

During experiment II, the markers were placed in the structure at two different levels (see Figure 8). As expected, it was observed that the markers located at higher levels have a lower chance of accumulating sediments. Besides this, the tilt angle of the marker affects the sediment accumulation and the detectability. This was the case with the ST-AM-43, (Figure 12h), which totally lost its detectability after 21 days of deployment. All important markers (ID: 28, 34, 35, 41, 42, 49) were placed on the upper level to have similar visibility. In terms of the external shape or the internal pattern of the enclosure, no significant impact on performance is appreciated.

After 50 days of deployment, we decided to leave the structure and see if, in the long run, the markers would survive. After five months, the marine growth fully covered the 3D-AM markers, making them non-detectable too.

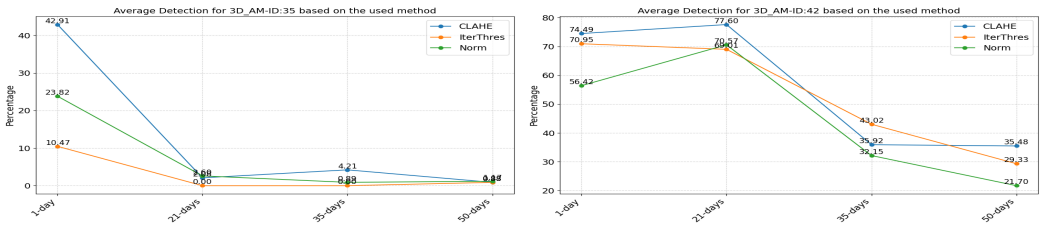

(**a**) 3D-AM-35 (**b**) 3D-AM-42

Figure 12. *Cont.*

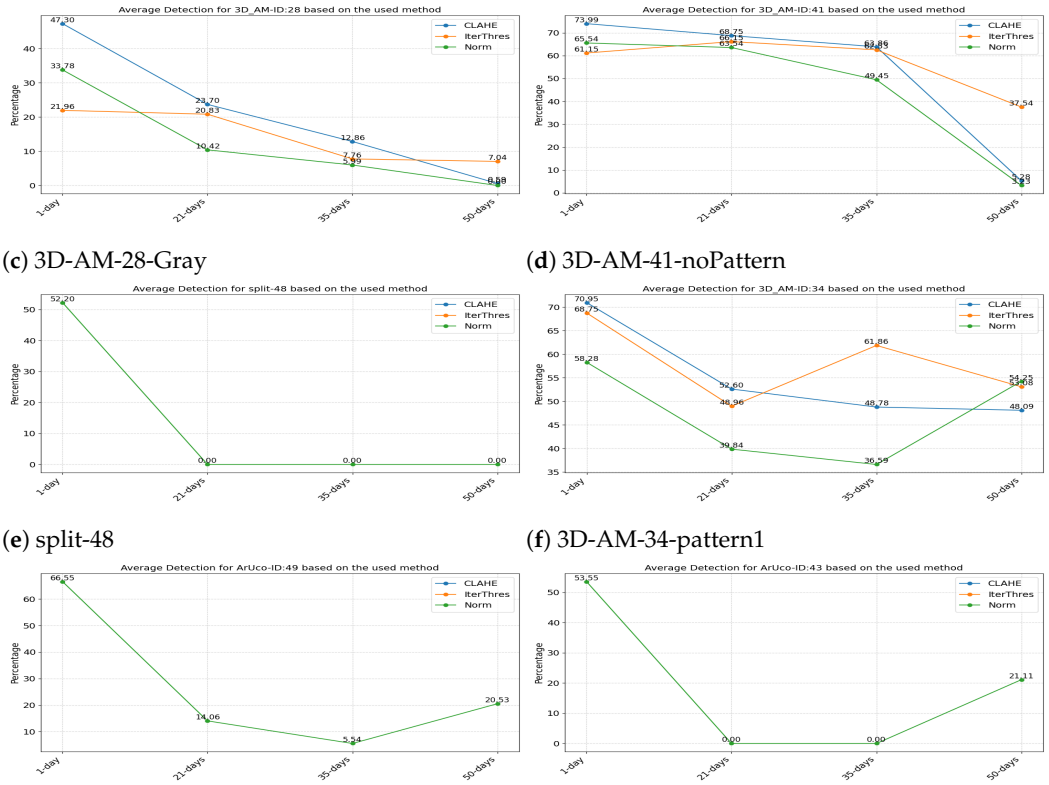

(**c**) 3D-AM-28-Gray (**d**) 3D-AM-41-noPattern

(**e**) split-48 (**f**) 3D-AM-34-pattern1

(**g**) ST-AM-49-30º (**h**) ST-AM-43-0º

Figure 12. The detection of each added marker on the structure, (**a**) is the old marker used in exp.1, (**c**) is a gray pattern and enclosure marker, (**b**,**d**,**e**) have different internal pattern, this is removed in the final design as its effect was minimal. (**f**) is a pattern with a background at 1 cm spacing, (**g**,**h**) are 3D-printed ArUco markers.

5.4.2. Detectability vs Range

Figure 13, details the percentage of marker detections according to distance for the five Three-Dimensional Binary Marker and the two Standard ArUco Marker. It can be appreciated that the detection of the standard markers was highly affected by the sediment accumulation (see Figure 13b,c), while the Three-Dimensional Binary Marker (ID:34-42) was still detectable at up to 5 m range. An inconsistent behaviour of Standard ArUco Marker detection degradation can be appreciated between Figure 13b–d.

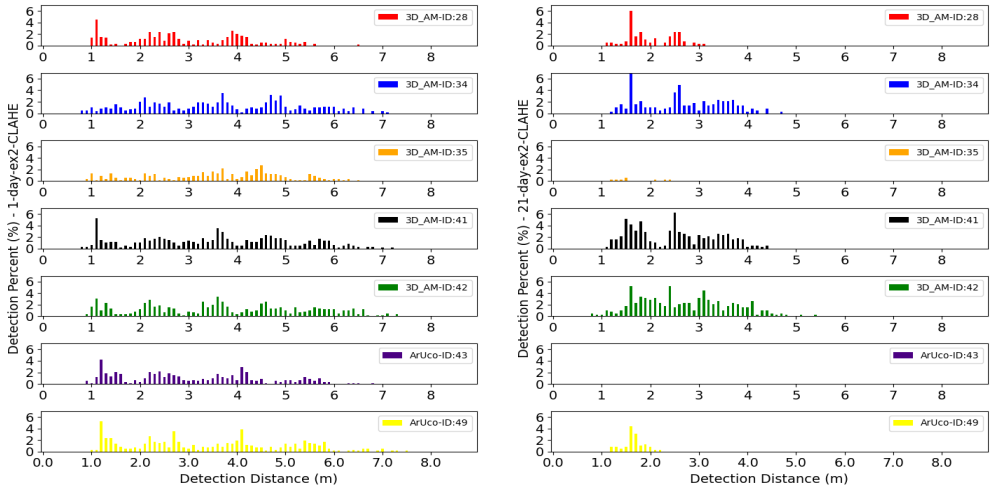

(**a**) 1st day (**b**) 21st day

Figure 13. *Cont.*

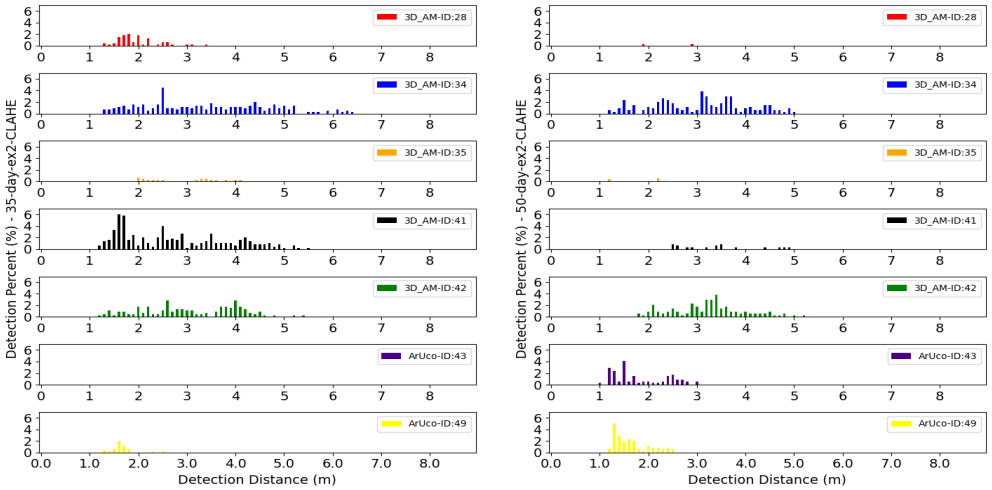

(**c**) 35th day (**d**) 50th day

Figure 13. The detection percentage in terms of the distance for the 3D-AM and the normal ArUcos.

After 35 days of deployment, the detection percentage dropped significantly, then after 50 days, it slightly recovered instead of being even more degraded as expected. Taking a close look at Figure 11b,c, we can deduce that something happened that slightly cleaned the markers. We do not know the exact origin, maybe the flow of a nearby ship's engine, but it's clear that it was due to an external agent.

5.4.3. Pre-Processing Method

Figure 14a shows the average detection, over all the datasets, for each pre-processing method used for detection of the 3D-AM markers. Figure 14b averages the detection of the five Three-Dimensional Binary Marker per collected dataset over a day. By only considering the 3D-AM-34 (pattern 1), 3D-AM-41 (no pattern), and 3D-AM-42 (pattern 2), the average detection percentages for the normalization, CLAHE, and the iterative threshold methods were 43.9%, 51.8%, and 54.3%. While their average execution times were Δt, $1.4 \sim 1.7\Delta t$ and $8.5 \sim 10.1\Delta t$ respectively, being Δt the lowest execution time of the three methods. The 3D-AM-28 (grey) marker and the former 3D-AM-35 (used in experiment I) markers were discarded, since their purpose was to check the color and size effect on the detection. Therefore, the best results were obtained using the iterative threshold method, followed by the CLAHE with a slightly inferior performance.

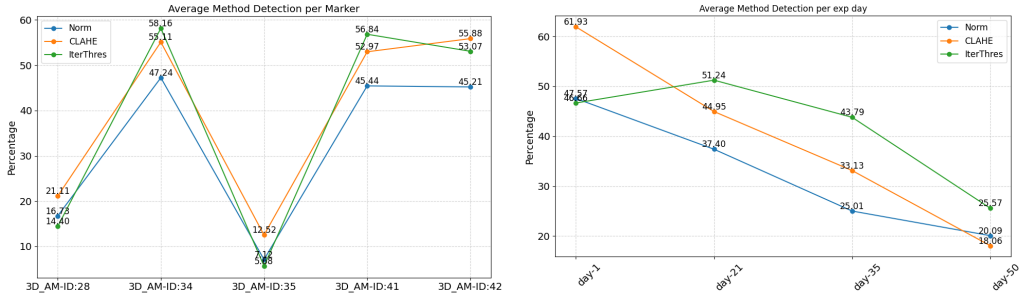

(**a**) Detection avg per marker (**b**) Detection avg per day

Figure 14. Average detection of the 3D-ArUco markers using the proposed methods.

6. Conclusions

This work has introduced the three-dimensional binary tag (3D-BM), a novel passive underwater marker designed to address the limitations of traditional 2D fiducial tags. The research included the design conceptualization, simulation validation, implementation, controlled water tank testing, and long-term sea trials. Key performance factors such as shape, size, internal pattern, and pre-processing algorithms have been evaluated. It has been shown that the marker's 3D geometry significantly improves visibility under sediment and biofouling buildup, improving its detection percentage.

In conclusion, the 3D-BM provides a durable and efficient solution for Long-Term Deployment. Its unique 3D design has successfully mitigated the challenges of sediment accumulation and marine growth that limit the functionality of conventional flat markers. The marker has been thoroughly validated through multi-stage experimentation, demonstrating superior detectability over time. By remaining compatible with existing fiducial detection algorithms and being easily manufacturable using 3D printing, the 3D-BM has offered a practical and scalable solution. Additionally, the use of enhanced image pre-processing has significantly improved detection rates.

In summary, the 3D-AM markers demonstrated good detectability in terms of distance and detection percentage. As the pattern uses holes to represent one of the binary colors, the contour of the binary pattern is visible regardless of the sediment accumulation. In contrast, the two-dimensional marker failed after only 20 days of deployment. Finally, after five months, all markers failed as they were fully covered by marine growth.

To extend the Three-Dimensional Binary Markers operational lifespan, we can evaluate anti-biofouling materials (e.g., aquasign [21] or other silicone-based coatings or 3D-printable copper composites [22]) in controlled marine trials, reducing the effect of biofouling and focusing more on the sediment accumulation. Additionally, we propose: (1) deep-sea validation or an artificial pit with the absence of light, and (2) benchmarking with other fiducial markers (AprilTag, STag) under standardized turbidity and light conditions, as this research only considered ArUco markers. These steps will bridge lab-to-field gaps, ensuring broader applicability for offshore infrastructure and AUV navigation.

Author Contributions: Conceptualization, P.C. and J.E.; Methodology, A.C., P.C., J.E., I.E. and P.R.; Software, A.C.; Formal analysis, A.C. and J.E.; Investigation, A.C.; Resources, J.E.; Writing—original draft, A.C.; Writing—review & editing, P.C., J.E. and P.R.; Supervision, J.E. and P.R. All authors have read and agreed to the published version of the manuscript.

Funding: This paper has been supported by the TANDEM Project (PLEC2023-149910OB-C31) and the COOPERAMOS Project (PID2020-115332RB-C32) funded by the Spanish Ministry of Science and Innovation. Beside the projects, Author Alaaeddine is a candidate of the Joan Oró Grants for the recruitment of predoctoral research staff in training: (2024 FI-3 00065)

Data Availability Statement: The recorded data are available on "https://doi.org/10.5281/zenodo.15749696". The detection code and marker designs are available on git@github.com:Alaashaarani/3D-binaryMarker.git.

Acknowledgments: We would like to thank Josep Forest, and Valerio Franchi for their recommendations during the development of the marker. And a special thanks to Nuno Gracias for his constant guidance and recommendations to achieve this research.

Conflicts of Interest: The funders had no role in the design of the study; in the collection, analyses, or interpretation of data; in the writing of the manuscript, or in the decision to publish the results.

Abbreviations

AUVs	Autonomous Underwater Vehicles
CLAHE	Contrast-Limited Adaptive Histogram Equalization
DS	Docking Station
IMR	Inspection, Maintenance, and Repair
LC-AM	Laser-Cut ArUco Marker
ROV	Remotely Operated Vehicle
ST-AM	Standard ArUco Marker
TRL	Technology Readiness Level
3D-BM	Three-Dimensional Binary Marker
3D-AM	Three-Dimensional ArUco Marker
UM	Underwater Marker
LTD	Long-Term Deployment
UUVs	Underwater Unmanned Vehicles

References

1. Ridao, P.; Carreras, M.; Ribas, D.; Sanz, P.J.; Oliver, G. Intervention AUVs: The next challenge. *Annu. Rev. Control* **2015**, *40*, 227–241. [CrossRef]
2. Garrido-Jurado, S.; Muñoz-Salinas, R.; Madrid-Cuevas, F.J.; Marín-Jiménez, M.J. Automatic generation and detection of highly reliable fiducial markers under occlusion. *Pattern Recognit.* **2014**, *47*, 2280–2292. [CrossRef]
3. Olson, E. AprilTag: A robust and flexible visual fiducial system. In Proceedings of the 2011 IEEE International Conference on Robotics and Automation, Shanghai, China, 9–13 May 2011; pp. 3400–3407. [CrossRef]
4. Bosch, J.; Gracias, N.; Ridao, P.; Istenič, K.; Ribas, D. Close-Range Tracking of Underwater Vehicles Using Light Beacons. *Sensors* **2016**, *16*, 429. [CrossRef] [PubMed]
5. Ghosh, S. Comparative study of noise between underwater active and passive markers. In Proceedings of the 2014 International Conference on Communication and Signal Processing, Melmaruvathur, India, 3–5 April 2014; pp. 1552–1556. [CrossRef]
6. Jurado-Rodriguez, D.; Muñoz-Salinas, R.; Garrido-Jurado, S.; Romero-Ramirez, F.J. Planar fiducial markers: A comparative study. *Virtual Real.* **2023**, *27*, 1733–1749. [CrossRef]
7. Kalaitzakis, M.; Cain, B.; Carroll, S.; Ambrosi, A.; Whitehead, C.; Vitzilaios, N. Fiducial Markers for Pose Estimation. *J. Intell. Robot. Syst.* **2021**, *101*, 71. [CrossRef]
8. Kato, H.; Billinghurst, M. Marker tracking and HMD calibration for a video-based augmented reality conferencing system. In Proceedings of the 2nd IEEE and ACM International Workshop on Augmented Reality (IWAR'99), San Francisco, CA, USA, 20–21 October 1999; pp. 85–94. [CrossRef]
9. Benligiray, B.; Topal, C.; Akinlar, C. STag: A stable fiducial marker system. *Image Vis. Comput.* **2019**, *89*, 158–169. [CrossRef]
10. Saipem. Available online: https://www.saipem.com/en (accessed on 23 July 2025).
11. Qu, J.; Xie, J.; Su, T.; Li, X.; Zhang, J.; Sun, Q.; Jiao, H. Autonomous docking system for UUV based on cooperative guidance of multiple markers: Design and experiment. *Ocean. Eng.* **2024**, *313*. [CrossRef]
12. Volden, Ø.; Stahl, A.; Fossen, T.I. Vision-based positioning system for auto-docking of unmanned surface vehicles (USVs). *Int. J. Intell. Robot. Appl.* **2022**, *6*, 86–103. [CrossRef]
13. Chen, J.; Sun, C.; Zhang, A. Autonomous Navigation for Adaptive Unmanned Underwater Vehicles Using Fiducial Markers. In Proceedings of the 2021 IEEE International Conference on Robotics and Automation (ICRA 2021), Xi'an, China, 30 May 2021–5 June 2021. [CrossRef]
14. Chavez, A.G.; Mueller, C.A.; Doernbach, T.; Birk, A. Underwater navigation using visual markers in the context of intervention missions. *Int. J. Adv. Robot. Syst.* **2019**, *16*, 1729881419838967. [CrossRef]
15. Wei, Q.; Yang, Y.; Zhou, X.; Fan, C.; Zheng, Q.; Hu, Z. Localization Method for Underwater Robot Swarms Based on Enhanced Visual Markers. *Electronics* **2023**, *12*, 4882. [CrossRef]
16. dos Santos Cesar, D.B.; Gaudig, C.; Fritsche, M.; dos Reis, M.A.; Kirchner, F. An Evaluation of Artificial Fiducial Markers in Underwater Environments. In Proceedings of the OCEANS 2015-Genova, Genova, Italy, 18–21 May 2015; pp. 1–6. [CrossRef]
17. Ren, Z.; Lensgraf, S.; Li, A.Q. Improving the Perception of Visual Fiducial Markers in the Field Using Adaptive Active Exposure Control. In Proceedings of the Experimental Robotics, ISER 2023, 18th International Conference on Experimental Robotics (ISER), Chiangmai, Thailand, 26–30 November 2023; pp. 274–284. [CrossRef]
18. Jung, K.; Youn, P.; Choi, S.; Lee, J.; Kang, H.J.; Myung, H. Development of retro-reflective marker and recognition algorithm for underwater environment. In Proceedings of the 2017 14th International Conference on Ubiquitous Robots and Ambient Intelligence (URAI), Jeju, Republic of Korea, 28 June 2017–1 July 2017; pp. 666–670. [CrossRef]

19. Čejka, J.; Bruno, F.; Skarlatos, D.; Liarokapis, F. Detecting Square Markers in Underwater Environments. *Remote Sens.* **2019**, *11*, 459. [CrossRef]
20. Cesar, D.; Joyeux, S.; Reis, M.; Conceição, A.; Albiez, J. Improvement of visual servoing tasks by underwater image enhancement. In Proceedings of the OCEANS 2017-Anchorage, Anchorage, AK, USA, 18–21 September 2017; pp. 1–6.
21. Aquasign. Offshore Technology. 2022 Available online: https://www.offshore-technology.com/contractors/subsea/aquasign/ (accessed on 23 July 2025).
22. Cui, L.; Cheng, C.; Li, X.; Gao, X.; Lv, X.; Wang, Y.; Zhang, H.; Lei, K. Comprehensive assessment of copper's effect on marine organisms under ocean acidification and warming in the 21st century. *Sci. Total Environ.* **2024**, *927*, 172145. [CrossRef] [PubMed]
23. Bennett, L.E.; Drikas, M. The evaluation of colour in natural waters. *Water Res.* **1993**, *27*, 1209–1218. [CrossRef]
24. IAC Acoustics. 2024. Available online: https://www.iacacoustics.global/anechoic-chambers/anechoic-chambers/ (accessed on 23 July 2025).
25. Open Source Computer Vision Library. 2025. Available online: https://opencv.org/ (accessed on 23 July 2025).
26. Cejka, J.; Zuzi, M.; Agrafiotis, P.; Skarlatos, D.; Bruno, F.; Liarokapis, F. *Improving Marker-Based Tracking for Augmented Reality in Underwater Environments*; The Eurographics Association: Liverpool, UK, 2018. [CrossRef]
27. Otsu, N. A Threshold Selection Method from Gray-Level Histograms. *IEEE Trans. Syst. Man Cybern.* **1979**, *9*, 62–66. [CrossRef]
28. Soille, P., Erosion and Dilation. In *Morphological Image Analysis: Principles and Applications*; Springer: Berlin/Heidelberg, UK, 2004; pp. 63–103. [CrossRef]
29. Community, B.O. *Blender-A 3D Modelling and Rendering Package*; Blender Foundation, Stichting Blender Foundation: Amsterdam, The Netherlands, 2018.

Disclaimer/Publisher's Note: The statements, opinions and data contained in all publications are solely those of the individual author(s) and contributor(s) and not of MDPI and/or the editor(s). MDPI and/or the editor(s) disclaim responsibility for any injury to people or property resulting from any ideas, methods, instructions or products referred to in the content.